# Chapter 6
# Research on Soot Filtration and Pressure Drop Characteristics of DPF

**Ying Gao, Hongqi Liu, Wei Chen, Tieqiang Fu, Maodong Fang and Jun Li**

**Abstract**  An integrated DPF filtration model is proposed to study the properties of soot filtration and pressure drop, which includes deep bed filtration model, cake filtration model and pressure drop model. Research results show that the evolution of filtration can be divided into two stages named as deep bed filtration and cake filtration respectively. During deep bed filtration, soot is trapped in the filter wall, which results a rapid pressure drop gradient of 7.6 Pa/s. However, the soot quality only accounts for 1.6% of the total in whole filtration process. Compact soot layer is developed during soot filtration. And a linear increase of pressure drop with the gradient of 1.4 Pa/s during the stage. Besides, the pressure drop caused by the soot layer and cake layer are 54 and 38% respectively in the whole simulation duration.

**Keywords**  DPF · Deep bed filtration · Cake filtration · Pressure drop

## 6.1  Introduction

As a valid method, DPF is widely used in the diesel vehicle to decrease soot emission. With soot loading increasing, the pressure drop increases at the same time, which will reduce the engine performance. To decrease pressure drop, soot regeneration is needed. By studying the substrate filtrating characteristics, the theoretical foundation is set up to predict the suitable time for regeneration. A visual experimental research has been made to research the characteristics of soot filtration in wall surface and inside the wall by Shigeki [1]. Filtration characteristics in different loading conditions were studied by Xiong Chen [2].

Y. Gao (✉) · H. Liu · W. Chen · J. Li
State Key Laboratory of Automotive Simulation and Control,
Jilin University, Changchun, China
e-mail: gaoying@jlu.edu.cn

T. Fu · M. Fang
China Automotive Technology and Research Center, Tianjin, China

Deep bed filtration and cake filtration models have been used to analysis the characteristics of pressure drop, filtration process and soot mass in this paper. Further, soot distribution and the impact of soot mass to pressure has been studied with pressure drop model.

## 6.2 Modeling of Soot Filtration

The filtration process of porous wall DPF includes deep bed filtration and cake filtration [3], which is showed in Fig. 6.1. Because of the large numbers and similar of channels, the specific characteristics of DPF are studied based on a single inlet and outlet like schematic Fig. 6.2.

Three substrate mechanisms are assumed when modeling DPF filtration models. First, particles are collected through Brownian diffusion and interception while interception is ignored. Second, to treat the soot in substrate distributed average. Last, to hold the velocity of the exhaust in filter wall is a constant and the physics parameters are the same in clean substrate.

### 6.2.1 Deep Bed Filtration Model

To study the deep bed filtration process, the filter wall is divided into a few slabs, while model of spherical cell is used in each slab [4]. Defining the spherical unit collector of diameter is b and the diameter of collector is dc. The deep bed slabs and the collector are showed in Figs. 6.3 and 6.4, respectively.
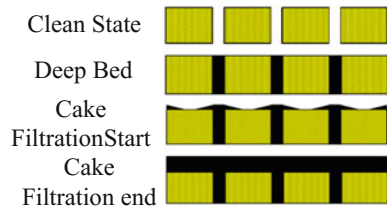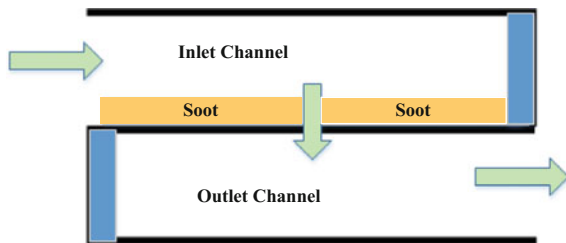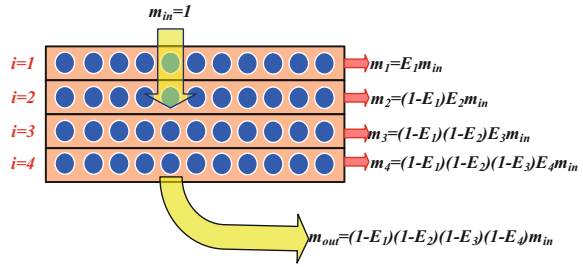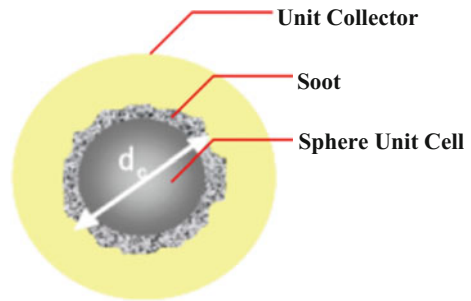


**Fig. 6.1** DPF filtration process

Clean State

Deep Bed

Cake FiltrationStart

Cake Filtration end



**Fig. 6.2** DPF single inlet and oulet

Inlet Channel

Soot          Soot

Outlet Channel

**Fig. 6.3** Schematic of deep bed divided into slabs for computational purposes



**Fig. 6.4** Schematic diagram of spherical collective unit



Soot mass in the deep bed is calculated by Eq. (6.1):

$$m_{wall}(t) = \sum_{i=1}^{N} [m(i-,t)E(i-,t1)] \tag{6.1}$$

where

$N$     number of divided slabs for deep bed
$i$     serial number of slabs
$E(i)$     collection efficiency for different slabs

Wall collection efficiency is critical to study the retained soot mass. For clean porous wall DPF, the initial collector size $d_{c0}$ and the spherical unit collector of diameter b are defined by Eqs. (6.2) and (6.3):

$$d_{c0} = \frac{3(1 - \varepsilon_0)}{2\varepsilon_0} d_{pore} \tag{6.2}$$

$$b = \left( \frac{d_{c0}^3}{1 - \varepsilon_0} \right)^{\frac{1}{3}} \tag{6.3}$$

where

$d_{pore}$     diameter of the pore in filter wall

$\varepsilon_0$      initial porosity, which is set 0.59 in this paper

Particles are trapped by only one mechanism of Brownian diffusion or interception in the same time [5]. Then, overall collection efficiency for a single collector can be given by Eq. (6.4):

$$\eta_{DR} = \eta_D + \eta_R - \eta_D\eta_R \tag{6.4}$$

where

$\eta_D$     Brownian diffusion collective efficiency, $\eta_D = 3.5 \cdot g(\varepsilon) \cdot Pe^{-\frac{2}{3}}$

$\eta_R$     direct interception collective efficiency, $\eta_R = 1.5N_R^2 \frac{(g(\varepsilon))^3}{(1+N_R)^{\frac{3-2\varepsilon}{3\varepsilon}}}$

$N_R$    Dimensionless interception parameter

$Pe$    Peclet Number, which is a dimensionless number that measures the relation between convective and diffusive motion of particles flowing to the surface of a collector [6]

$g(\varepsilon)$    Kuwabara's hydrodynamic factor, which is calculated by Eq. (6.5):

$$g(\varepsilon) = \left[ \frac{\varepsilon}{2 - \varepsilon - \frac{9}{5}(1-\varepsilon)^{\frac{1}{3}} - \frac{1}{5}(1-\varepsilon)^2} \right]^{\frac{1}{3}} \tag{6.5}$$

The initial value of clean filter wall collective efficiency is expressed in Eq. (6.6):

$$E = 1 - \exp\left[ -\frac{3\eta_{DR} \cdot (1-\varepsilon_0) \cdot w_s}{2\varepsilon_0 d_{c0}} \right] \tag{6.6}$$

With the filtration of deep bed, soot will deposit in the spherical collector unit and form a large unit until the unit diameter reach b. Because of the difference of particles mass retained in different slabs of the filter wall, which is resulted of different flow direction of permeated gas, the diameter of collector, porosity of the substrate and collective efficiency are varied with time. And the collective efficiency in different slabs are calculated by Eq. (6.7):

$$E(i,t) = 1 - \exp\left[ -\frac{3\eta_{DR}(i,t) \cdot (1-\varepsilon(i,t)) \cdot (x_{i+1} - x_i)}{2\varepsilon(i,t)d_c(i,t)} \right] \tag{6.7}$$

The mode of soot filtration will finally turn to cake filtration after deep bed filtration. So the end time of substrate trap is a key parameter. It can help analyzing the retained soot mass in filter and the increase rate of pressure drop during deep bed filtration. By analyzing the physics system of the filter wall, the cake layer comes into being when the first discrete slab reach the maximum trapping mass. The maximum mass of the first discrete slab is calculated by Eq. (6.8):

$$m_{1\max} = \frac{\rho_{soot,wall}\pi N_{collector}\left[(\psi b)^3 - d_{c0}^3\right]}{6} \tag{6.8}$$

where

$\rho_{soot,wall}$ density of the soot in the filter wall

$N_{collector}$ number of collector

$\psi$ a dimensionless 'percolation' control constant $(0 < \psi < 1)$ [7].

### 6.2.2 Cake Filtration Model

After entering the cake layer filtration, the particles begin to form a dense cake layer on the wall surface. And because of the gradual formation of the soot accumulation and filter cake layer, the trapping effect in cake layer is higher than the deep bed filtration rate. Based on the mass balance mechanism of soot filtration process, the soot mass should be satisfied Eq. (6.9):

$$\frac{dm_{sc}(z)}{dt} = +\dot{R}_{sc} + v_w(z) \cdot \dot{m}_{soot,inl} \cdot S_{sc} \tag{6.9}$$

where

$m_{sc}(z)$ total soot mass in DPF

$\dot{R}_{sc}$ reaction caused by source term

$v_w(z)$ dimensionless flow rate

$S_{sc}$ two sources conversion term expressing the start of cake layer collection

Further, the thickness of cake layer is calculated by Eq. (6.10):

$$w_s = \frac{\alpha - \sqrt{\alpha^2 - \frac{m_c}{N_{cell}L\rho_{soot,c}}}}{2} \tag{6.10}$$

where

$\alpha$ width of DPF, which is set 1.5 mm

$m_c$ overall retained soot mass

$N_{cell}$ number of inlet cell

L filter length, which is set 203.2 mm

$\rho_{soot,c}$ density of the cake layer soot.

### 6.2.3  Pressure Drop Model

In view of the characteristics of DPF structure, the pressure drop is mainly caused by six parts. That includes pressure drop when the exhaust gas flow through cake layer and wall, the pressure drop caused by the resistance in the inlet and outlet channels, the pressure drop caused by the mutation of the DPF import and export circulation section [6]. Then, the total pressure drop of a loaded filter is obtained by summing up above mentioned and shown in Eq. (6.11):

$$
\begin{aligned}
\Delta P &= \Delta P_{wall} + \Delta P_{soot} + \Delta P_{inlet} + \Delta P_{outlet} + \Delta P_{cont\,\&\,exp} \\
&= \frac{\mu}{k_{wall}} \frac{U\alpha}{4L} w + \frac{\mu}{k_{soot}} \int_0^w u(x)dx + \frac{\mu FUL}{3}\left[\frac{1}{(\alpha - 2w_s)^2} + \frac{1}{\alpha^2}\right] + \zeta \frac{\rho U^2}{2} \\
&= \frac{\mu Q}{2V_{trap}}(\alpha + w)^2 \left[\frac{w_s}{k_w \alpha} + \frac{1}{2k_{soot}}\ln\left(\frac{\alpha}{\alpha - 2w_s}\right) + \frac{4FL^3}{3}\left(\frac{1}{(\alpha - 2w_s)^4} + \frac{1}{\alpha^4}\right)\right] \\
&\quad + \frac{\rho Q^2(\alpha + w_s)^4}{V_{trap}^2 \alpha^2} 2\xi \left(\frac{L}{\alpha}\right)^2
\end{aligned}
$$

$$(6.11)$$

where

| | |
|---|---|
| $Q$ | exhaust flow volume |
| $W$ | wall thickness equal to 0.3048 mm |
| $w_s$ | thickness of the soot layer |
| $k_{wall}$ | wall permeability |
| $k_{soot}$ | cake layer permeability |
| $\mu$ | exhaust dynamic viscosity |
| $\rho$ | exhaust gas density |
| $\zeta$ | resistance coefficient. |

## 6.3  Parameter Calibration and Verification of Models

To calibrate the key parameters in model based on experiment data, which are wall surface permeability in clean DPF, wall surface permeability after soot loaded, density of soot, wall surface permeability in cake layer, respectively. And the results of calibration are $k_0 = 2.06 \times 10^{-13}(m^2)$, $k_{wall} = 5.02 \times 10^{-14}(m^2)$, $\rho_{soot,c} = 218(kg/m^3)$, $k_{soot} = 3.92 \times 10^{-15}(m^2)$. The pressure drop, which is calculated by the model applied with the parameters after calibration, is compared with the experiment data, and the difference value is showed in Figs. 6.5 and 6.7, while the relative error is showed in Figs. 6.6 and 6.8.
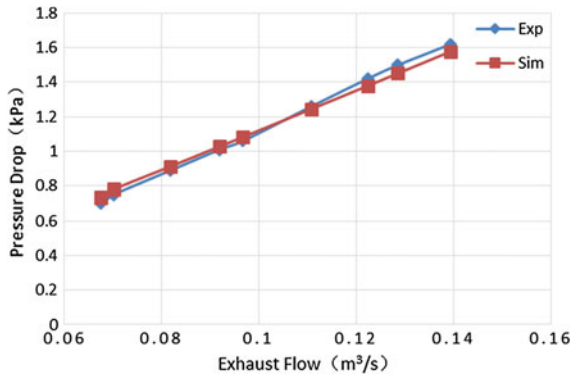
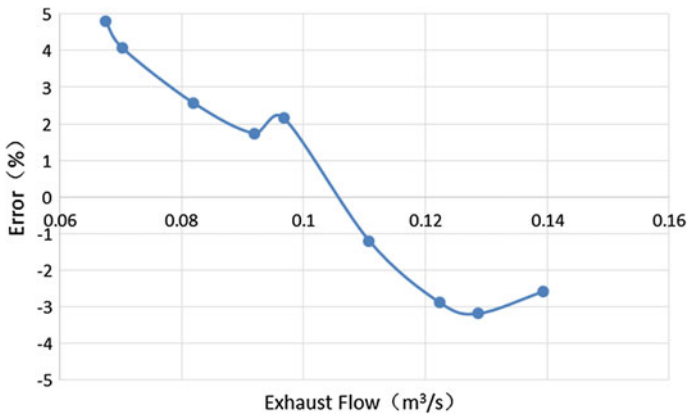**Fig. 6.5** Relation between pressure drop and exhaust mass flow in clean DPF
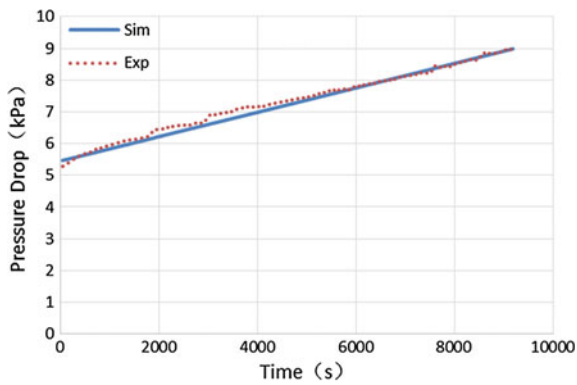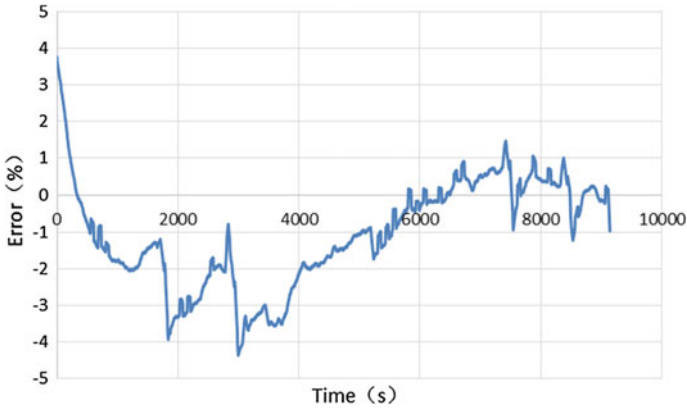


**Fig. 6.6** Relative error



**Fig. 6.7** Variation of pressure drop in filtration process

**Fig. 6.8** Relative error

The relative error between simulation results and experiment data is within ±5%. Results show that the simulation models can be used to study the characteristics of the filter in follow-on work.

## 6.4 Characteristics Analysis of Soot Filtration

### 6.4.1 Characteristics Variation of Pressure Drop

It can be seen from Fig. 6.9 that the duration of deep bed filtration phase is 185 s and change gradient of pressure drop is 7.6 Pa/s. And the duration of cake layer filtration phase is 1657 s and change gradient of pressure drop is 1.4 Pa/s in the whole filtration process of DPF. Thus, the degree of pressure drop is greater in deep bed filtration stage than in cake filtration stage with a shorter duration oppositely. As shown in Fig. 6.10, deep-bed filtration occurs inside the wall of DPF, which lead to the decrease of wall surface permeability. The permeability ratio of first discrete layer is minimum of $7.34 \times 10^{-14}$ (m$^2$) after deep-bed filtration phase, which finally causes that the quantities of pressure drop in wall surface accounts for 78% of whole pressure drop. With the beginning of cake layer filtration, the ratio of pressure drop is increased linearly. And the proportion of pressure drop in soot layer is increased gradually while the one in wall surface and inlet/outlet channels is decreased gradually. By the end of soot filtration, the proportions of pressure drop in soot layer, wall surface and inlet/outlet channels are 54, 38 and 8% of the whole pressure drop respectively.

**Fig. 6.9** Variation of
pressure drop in process of
soot filtration
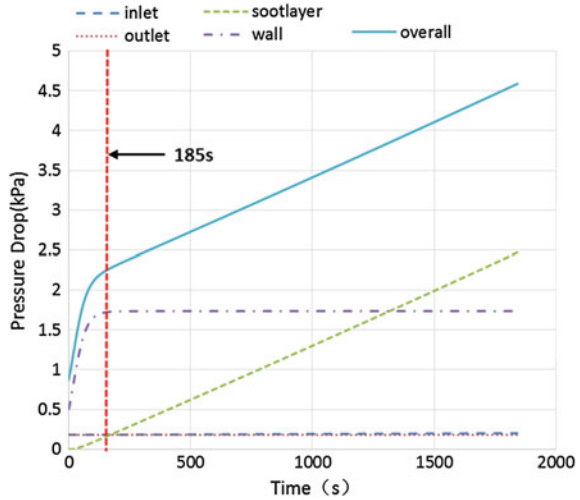


**Fig. 6.10** Distribution ratio
of pressure drop
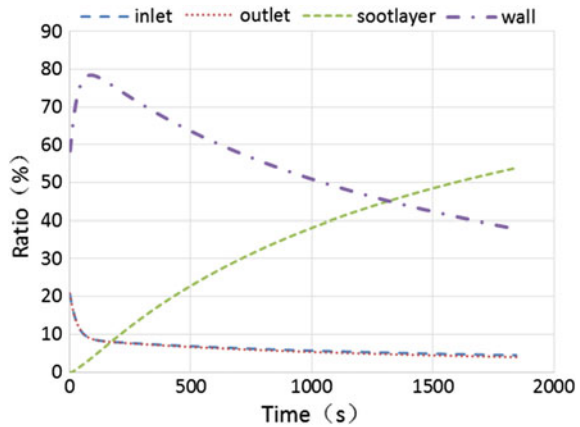


## 6.4.2   Soot Mass Distribution Characteristics

As shown in Fig. 6.11, the retained soot mass is 25 g in filter, while the filtered soot
mass retained in wall surface is 0.42 g. And the proportion of soot mass is 1.68% in
deep bed filtration stage. It can be seen from Fig. 6.12, the soot mass is decreased
along the direction of gas flow, while the soot mass in the first layer of wall surface
have a maximum value of 66% of retained soot mass in deep bed. The soot mass is
increased linearly in cake layer filtration and the final soot mass is 24.6 g. That
accounts 98.4% of soot mass in the filter.

**Fig. 6.11** Variation of soot mass
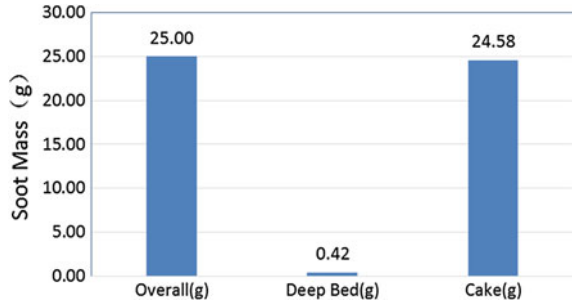


**Fig. 6.12** Distribution of soot in different layer of wall surface
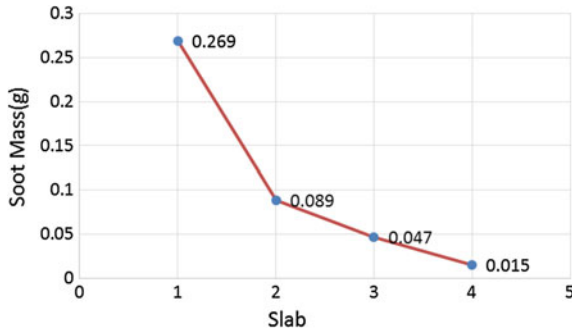


## 6.5  Conclusions

(1) The integrated model have been built and verified with experiment data. The relative error is within ±5% between simulation results and experiment data.

(2) The pressure drop in deep bed filtration holds a dominant amount of pressure drop in DPF. The change rate is 7.6 Pa/s during this stage, and the soot mass filtered in deep bed is 1.68%. The pressure drop is linear increase with soot mass in cake layer filtration. And it's proportion is 54% of whole pressure drop with a longer duration than that in deep bed filtration time. The soot mass in the first layer of wall surface have a maximum value of 66% of retained soot mass in deep bed. The soot mass is increased linearly in cake layer filtration, and it accounts 98.4% of soot mass in the filter.

# References

1. Daido S, Nobuyuki T (2009) Visualization of the PM deposition and oxidation behavior inside the DPF wall [C]. SAE Paper, 2009-01-1473
2. Chen X, Li M, Hou X et al (2013) A study on the filtration characteristics of DPF for diesel vehicle particulates in different driving conditions [J]. Automot Eng 35(12):1074–1077
3. Choi S, Kyeong L (2013) Detailed investigation of soot deposition and oxidation characteristics in a diesel particulate filter using optical visualization [C]. SAE Paper, 2013-01-0528
4. Kiran C. Premchand, John H. Johnson, Song-Lin Yang (2009) Development of a 1-D CPF model to simulate active regeneration of a diesel particulate filter, SAE 2009-01-1283
5. Ohara E, Mizuno Y, Miyairi Y, et al (2007) Filtration behavior of diesel particulate filters (1) [C]. SAE Paper, 2007-01-0921
6. Konstandopoulos AG, Kostoglou M, Skaperdas E, et al (2000) Fundamental studies of diesel particulate filters: transient loading, regeneration and aging [C]. SAE Paper 2000-01-1016
7. Konstandopoulos AG (1999) Deposit growth dynamics: particle sticking and scattering phenomena. J Power Tech 109(1):262–277